Shubnikov–de Haas effect in low-stage acceptor-type graphite intercalation compounds

V. A. Kulbachinskii, S. G. Ionov, and S. A. Lapin
Low Temperature Physics Department, Moscow Lomonosov University, 119899 Moscow, Russia

A. de Visser*
Van der Waals–Zeeman Laboratory, University of Amsterdam, Valckenierstraat 65, 1018 XE Amsterdam, The Netherlands
(Received 9 November 1994)

Low-stage acceptor-type graphite intercalation compounds (GIC's) have been synthesized with intercalants Br_2, ICl, $CuCl_2$, $AlCl_3$, $FeCl_3$, ICl_3, $AlCl_3Br$, $SbCl_5$, and H_2SO_4. For the GIC that could be prepared in high-quality quasi-single-crystalline form, the electronic parameters were investigated by means of magnetotransport and Hall-effect measurements in the temperature interval $1.4\ K < T < 4.2\ K$ and in high magnetic fields (up to 35 T). In low magnetic fields for all first-stage compounds and most second-stage compounds a single Shubnikov–de Haas (SdH) frequency was observed. The angular dependence of the SdH frequency revealed a nearly cylindrical Fermi surface. However, for the second-stage compounds $C_{16}ICl_{0.8}$ and $C_{18.6}AlCl_{3.4}$ a more complicated Fermi surface was observed. In the case of $C_{16}ICl_{0.8}$ the Fermi surface consists of two concentric cylinders, while for $C_{18.6}AlCl_{3.4}$ frequency beats of two close frequencies were observed, yielding a Fermi surface in the shape of an undulating cylinder. The undulated Fermi surface possibly originates from the interaction between carbon atoms in neighboring graphite layers separated by the intercalant. The experimental data are compared to the band-structure model proposed by Blinowski and co-workers.

I. INTRODUCTION

Over the past decade the intercalation of graphite has attracted much attention because it provides a powerful technique for the controlled variation of materials parameters. Up to the present, a wide variety of graphite intercalation compounds (GIC's) has been synthesized and characterized (Refs. 1 and 2). GIC's show a multiplicity of physical phenomena, among which superconductivity and magnetic order are perhaps the most alluring. In addition, GIC's offer wide possibilities to study charge transport in quasi-two-dimensional structures. The physical characteristics depend on many factors, like the nature of the intercalant (acceptor or donor type), the stage number N (i.e., the number of graphite layers between the nearest intercalant layers), and the method of synthesis.

Acceptor-type GIC's may be synthesized by the intercalation of halogens, interhalides, metal halides, or acids. Interestingly, these materials can have a very high electrical conductivity (in the hexagonal basal plane) at room temperature, which, in combination with a low specific weight, makes them potentially attractive for applications. Detailed knowledge of the electronic band structure of GIC's is of great importance for the explanation of the high conductivity and for the controlled search for GIC's with desirable physical properties. Comprehensive information about the band structure, the Fermi surface, the effective masses, and the carrier concentration is provided by the investigation of magnetic quantum oscillations at low temperatures, preferably over a wide range of magnetic fields. However, for such investigations macroscopic single crystals of sufficient quality must be available. The aim of the present paper is to report upon the synthesis of a series of high-quality quasi-single crystals of low-stage acceptor-type GIC's with intercalants Br_2, ICl, $CuCl_2$, $AlCl_3$, $FeCl_3$, ICl_3, $AlCl_3Br$, $SbCl_5$, and H_2SO_4, and the subsequent experimental characterization by means of electrical conductivity, the Shubnikov–de Haas (SdH) effect, and the Hall effect. Magnetotransport measurements have been performed in the temperature interval $1.4\ K < T < 4.2\ K$ and in magnetic fields up to 35 T.

II. SYNTHESIS AND EXPERIMENTAL TECHNIQUES

The samples were prepared by the intercalation of highly oriented pyrolytic graphite. The pure graphite, annealed at a temperature of 3300 K, is characterized by a basal-plane grain size of $\sim 10^5$ Å and an interlayer distance (along the c axis) d_0 of 3.356 Å. The misorientation angle of the grains with respect to the c axis was less than 1°. Before intercalation, the graphite specimens were washed in acetone and subsequently degassed in vacuum for 20 min at a temperature of 700 K.

The intercalants were prepared in various ways. ICl was produced by synthesis from the elements and purified by recrystallization from the melt. $CuCl_2$ was produced by dehydration of the crystalline hydrate $CuCl_2 \cdot 2H_2O$ in boiling sulfurchloride with subsequent distillation of excess $SOCl_2$. Purification of the anhydrous copper chloride was then carried out by distillation in a stream of dry chlorine at a temperature of 950 K. $AlCl_3$, $FeCl_3$, ICl_3, and $SbCl_5$ were produced by synthesis from the elements and refined by multiple distillation in a dry chlorine flow or in vacuum (in the case of $SbCl_5$). Pure Br_2 and H_2SO_4 were purchased.

GIC's containing ICl, $CuCl_2$, $AlCl_3$, $FeCl_3$, and ICl_3

TABLE I. Crystallographic parameters of the investigated first- ($N=1$) and second- ($N=2$) stage graphite intercalation compounds: d_i is the thickness of the intercalant layer, I_c is the c-axis repeat distance.

Chemical composition	N	d_i (Å)	I_c (Å)
$C_{9.3\pm0.1}AlCl_{3.4\pm0.1}$	1	9.54±0.01	9.54±0.01
$C_{9.5\pm0.2}AlCl_3Br_{0.6\pm0.1}$	1	9.77±0.01	9.77±0.01
$C_8H_2SO_4$	1	7.98±0.01	7.98±0.01
$C_{27.5\pm0.5}ICl_{3.0\pm0.1}$	2	6.89±0.01	10.24±0.01
$C_{24.5\pm0.5}SbCl_{5.0\pm0.1}$	2	9.36±0.01	12.71±0.01
$C_{16.2\pm0.2}Br_{2.0\pm0.1}$	2	7.03±0.01	10.38±0.01
$C_{16}ICl_{0.8}$	2	7.16±0.01	10.51±0.01
$C_{9.8\pm0.1}CuCl_{2.05\pm0.02}$	2	9.40±0.01	12.75±0.01
$C_{16.3\pm0.2}ICl_{1.10\pm0.03}$	2	7.12±0.01	10.47±0.01
$C_{12.0\pm0.1}FeCl_{3.0\pm0.1}$	2	9.40±0.01	12.75±0.01
$C_{18.6\pm0.2}AlCl_{3.4\pm0.1}$	2	9.48±0.01	12.83±0.01

were prepared by the vapor method in a two-zone quartz or glass ampoule in a chlorine atmosphere. When $AlCl_3$ was intercalated in a bromine atmosphere, aluminum chloride GIC's with different bromine concentrations were formed. Variation of the temperature gradient between intercalant and graphite yielded GIC's of different stoichiometries. The temperature gradient also prevents condensation of the intercalant on the surface of the samples. GIC's containing Br_2, $SbCl_5$ and H_2SO_4 were synthesized by the liquid-phase method. Most of the compounds were sensitive to moisture, and, therefore, the samples were kept in a hermetically sealed chamber filled with dried argon.

The prepared specimens were analyzed chemically and investigated by means of x-ray techniques. The resulting chemical composition, the stage number N, and the relevant lattice parameters, i.e., the thickness of the intercalant layer d_i and the c-axis repeat distance $I_c=d_i+(N-1)d_0$, where $d_0=3.35$ Å is the c-axis lattice parameter of graphite, are listed in Table I. These analysis methods gave no direct information about the possible defect structures. However, the high quality of the prepared single-crystalline specimens is assured by the detection of magnetic quantum oscillations at low temperatures.

In order to perform magnetotransport measurements, electrical leads (copper wires) were attached to the samples, under a protective argon atmosphere, using silver paint. The samples had barlike shapes with typical dimensions $5\times1\times0.5$ mm^3 (the c axis is directed perpendicular to the 5×1-mm^2 surface). Transverse magnetoresistance and Hall-effect measurements were performed, using standard four-point techniques, for a current directed in the basal plane and a magnetic field applied along the c axis. Measurements in low magnetic fields were performed using a superconducting solenoid ($B_{max}=6$ T). Measurements in high magnetic fields (up to 35 T) were carried out at the High Field Facility of the University of Amsterdam. This long-pulse magnet is capable of reaching fields up to 40 T with a total pulse duration of 1 s. In order to prevent eddy-current heating, the samples are immersed in liquid helium.

III. RESULTS

The Hall coefficient R_H of the prepared GIC's was measured in magnetic fields up to 6 T at liquid-helium temperatures. In this field and temperature range, R_H is constant and positive for all compounds. This confirms that the investigated GIC's are of the acceptor type. The resulting hole concentration for the investigated specimens, $n_H=1/eR_H$, is listed in Table II. For stage-1 compounds n_H is of the order of $(0.1-0.2)\times10^{26}$ m^{-3}, while for stage-2 compounds n_H amounts to $(1-3)\times10^{26}$ m^{-3}, i.e., roughly one order of magnitude larger. An exception is formed by the case of $C_{9.5}AlCl_3Br_{0.6}$, where the presence of additional Br leads to a considerable enhancement of the carrier concentration.

Most of the specimens showed pronounced quantum oscillations in the transverse magnetoresistance. Some typical results for the stage-1 compounds $C_{9.3}AlCl_{3.4}$, $C_{9.5}AlCl_3Br_{0.6}$, and $C_8H_2SO_4$ obtained at $T=4.2$ K are shown in Fig. 1. A common feature of the low-field Shubnikov–de Haas (SdH) oscillations of these stage-1 compounds and the stage-2 compounds $C_{16.3}ICl_{1.1}$,

TABLE II. Parameters of the energy spectrum of first ($N=1$) and second ($N=2$) graphite intercalation compounds. R_H is the Hall constant, n_H and n_{SdH} give the carrier (hole) concentration determined from R_H and the SdH oscillations, respectively, S is the extremal cross section of the Fermi surface, m^*/m_0 is the effective mass in units of the free-electron mass, γ_0 is the intraplane interaction parameter, and E_F is the Fermi energy.

Compound	N	R_H (10^{-6} m^3/C)	S (Å^{-2})	n_H (10^{26} m^{-3})	n_{SdH} (10^{26} m^{-3})	m^*/m_0	γ_0 (eV)	E_F (eV)
$C_{9.3}AlCl_{3.4}$	1	0.5	0.00104±0.00002	0.12	0.11	0.065±0.003	3.2	−0.12
$C_{9.5}AlCl_3Br_{0.6}$	1	0.017	0.0326±0.0003	3.6	3.4		3.2	−0.69
$C_8H_2SO_4$	1	0.27	0.00189±0.00002	0.23	0.23	0.070±0.002	3.2	−0.14
$C_{27.5}ICl_3$	2	0.022	0.0287±0.0003	2.8	2.9	0.148±0.008	2.4	−0.34
$C_{16}ICl_{0.8}$	2	0.016	0.0414±0.0003	3.9	3.9	0.187±0.007	2.5	−0.47
			0.0072±0.0003					
$C_{9.8}CuCl_2$	2	0.047	0.0162±0.0005	1.3	1.3	0.091±0.005	2.7	−0.25
$C_{16.3}ICl_{1.1}$	2	0.024	0.0272±0.0003	2.6	2.5	0.130±0.001	2.5	−0.34
$C_{12}FeCl_3$	2	0.025	0.0303±0.0003	2.5	2.4	0.145±0.007	2.7	−0.35
*$C_{18.6}AlCl_{3.4}$	2	0.023	0.0389±0.0005	2.7	2.8	0.15±0.03	2.5	−0.43
			0.0323±0.0005					

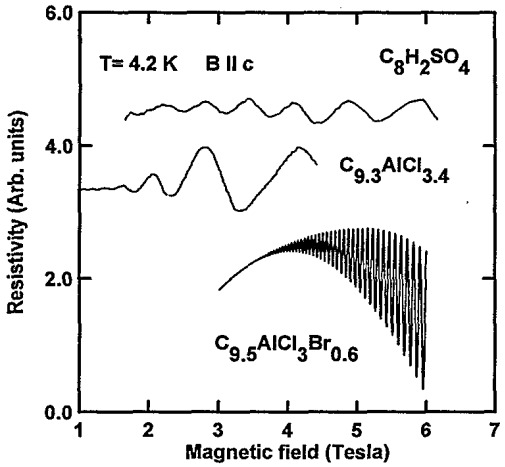

FIG. 1. Shubnikov–de Haas oscillations in the transverse magnetoresistance of the first-stage GIC's $C_8H_2SO_4$, $C_{9.3}AlCl_{3.4}$, and $C_{9.5}AlCl_3Br_{0.6}$ at $T=4.2$ K.

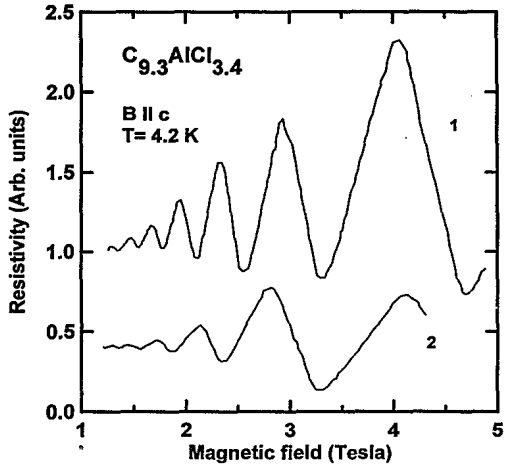

FIG. 2. Shubnikov–de Haas oscillations at $T=4.2$ K in the transverse magnetoresistance of the first-stage GIC $C_{9.3}AlCl_{3.4}$ before (1) and after (2) a two-day hold in helium atmosphere at room temperature.

$C_{9.8}CuCl_2$, $C_{12}FeCl_3$, and $C_{27.5}ICl_3$ is the monochromatic nature of the oscillations (one single frequency F), indicating the presence of only one extremal cross section of the Fermi surface S_F. By varying the angle θ between the applied field and the crystallographic c axis, it was found that $S_F(\theta)=S_F(0)/\cos\theta$, which confirms a nearly cylindrical Fermi surface in these GIC's. However, the amplitude of the SdH oscillations decreases rapidly with increasing θ, which limited the range of θ values for which it was possible to carry out the measurements to approximately 30°. The extremal Fermi-surface cross section $S_F(0)=(2\pi e/\hbar)F(0)$ (Ref. 3) of the investigated samples is listed in Table II. The hole concentrations deduced from the SdH oscillations, $n_{\mathrm{SdH}}=4S_F/\{(2\pi)^2 I_c\}$, are also listed in Table II, and are in good agreement with the ones determined from the Hall-effect measurements (n_H).

The sensitivity of the carrier concentration and, hence, the Fermi-surface cross section, of some compounds to the presence of the additional halogen is illustrated by the SdH signal of $C_{9.3}AlCl_{3.4}$ GIC's. After a two-day hold in helium atmosphere the extremal cross section decreased from 0.001 04 to 0.000 81 Å^{-2} (see Fig. 2), while the lattice parameters did not change. This can be explained by the evaporation of additional chlorine from the intercalated layers, as confirmed by chemical analysis.

For some specimens the SdH signal was investigated in high magnetic fields up to 35 T. In Fig. 3, the oscillatory part of the transverse magnetoresistance of the second-stage GIC's $C_{18.6}AlCl_{3.4}$ and $C_{9.8}CuCl_2$ is shown. The corresponding Fourier transforms are shown in Fig. 4. In the SdH oscillations of $C_{18.6}AlCl_{3.4}$, frequency beats are seen, yielding evidence for two close frequencies (338 and 408 T) of different amplitudes. In the Fourier transform two frequencies appear in the fundamental and first harmonic peaks. In the case of $C_{9.8}CuCl_2$, up to five harmonics of the fundamental frequency (170 T) appear in the Fourier transform. No frequency beating was observed. Peak splitting is visible for $C_{18.6}AlCl_{3.4}$ at $T=4.2$ K in fields exceeding 26 T (see Fig. 3). In the case of $C_{9.8}CuCl_2$, peak splitting is not obvious at $T=4.2$

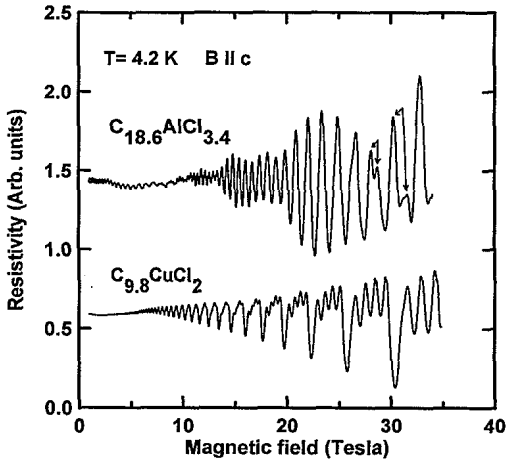

FIG. 3. Shubnikov–de Haas oscillations in the transverse magnetoresistance of the second-stage GIC's $C_{18.6}AlCl_{3.4}$ and $C_{9.8}CuCl_2$ at $T=4.2$ K. The connected arrows indicate peak splitting (see text).

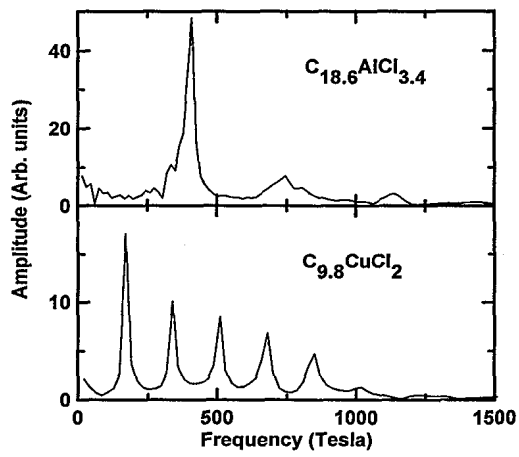

FIG. 4. Fourier transforms of the SdH oscillations of $C_{18.6}AlCl_{3.4}$ and $C_{9.8}CuCl_2$ ($T=4.2$ K).

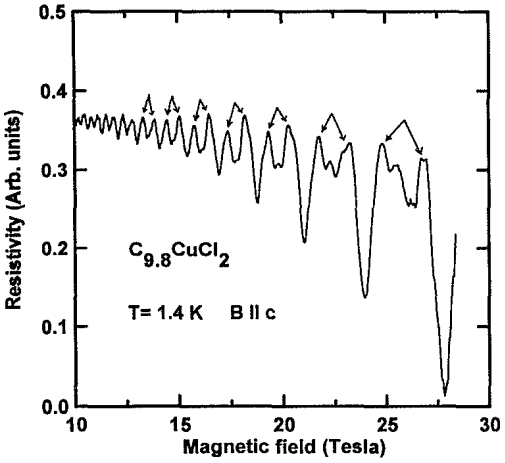

FIG. 5. Shubnikov–de Haas oscillations in the transverse magnetoresistance of the second-stage GIC $C_{9.8}CuCl_2$ at $T=1.4$ K. The connected arrows indicate peak splitting (see text).

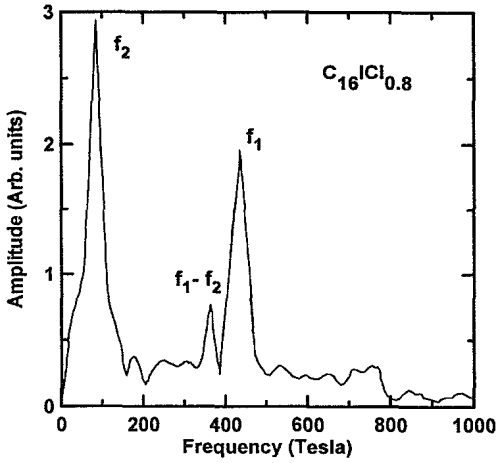

FIG. 7. Fourier transform of the SdH oscillations of $C_{16}ICl_{0.8}$ ($T=4.2$ K).

K, due to the high amplitude of the harmonics of the main frequency. However, when lowering the temperature to 1.4 K, peak splitting becomes clearly visible in fields exceeding 10 T (see Fig. 5). We attribute the peak splitting to spin splitting. The positions of the peaks due to spin-up and spin-down in magnetic field are marked by the connected arrows in Figs. 3 and 5. As is well known (Ref. 3), the energy distance between the Landau levels is given by $\Delta\epsilon_0=\hbar\omega_c$, where ω_c is the cyclotron frequency, and the spin splitting is given by $\Delta\epsilon_s=g\mu_B H$, where g is the g factor and μ_B is the Bohr magneton. The ratio of spin splitting (that is, the distance between two levels with spin-up and spin-down belonging to the same Landau level, marked by the connected arrows in Figs. 3 and 5) to the orbital splitting (the distance between the nearest Landau levels) is $\gamma=\Delta\epsilon_0/\Delta\epsilon_s=(1/2)g(m^*/m_0)$. From our experimental data γ amounts to ≈ 0.37 and ≈ 0.45 for $C_{9.8}CuCl_2$ and $C_{18.6}AlCl_{3.4}$, respectively.

SdH oscillations for the stage-2 GIC $C_{16}ICl_{0.8}$ are shown in Fig. 6, while the corresponding Fourier transform is shown in Fig. 7. Here we observed two distinctly different frequencies, a low frequency $f_2=76$ T and a high frequency $f_1=434$ T, which are connected to different sheets of the Fermi surface (see Sec. IV B).

In the case of the stage-2 GIC $C_{24.5}SbCl_5$ a complicated Fourier spectrum was observed, which depended on the cooling rate. For rapidly cooled samples many SdH frequencies were observed. A similar result was previously reported by Yosida and Tanuma (Ref. 4). Conversely, for slowly cooled samples, only two frequencies are observed, which arise from the basic graphite bands. The complicated Fourier spectrum of the SdH oscillations in the rapidly cooled case might be explained[5,6] by a freezing-in of the high-temperature structure of the intercalate. For the slowly cooled samples the intercalant structure is incommensurate with the graphite lattice, and thus one expects to observe only frequencies connected to the basic graphite bands. The present data for $C_{24.5}SbCl_5$ basically confirm the measurements previously reported in Refs. 4–8.

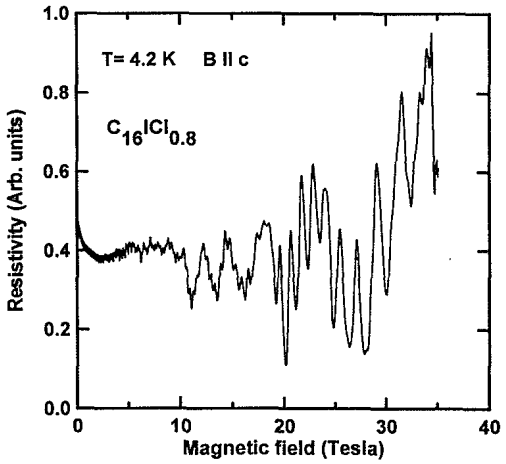

FIG. 6. Shubnikov–de Haas oscillations in the transverse magnetoresistance of the second-stage GIC $C_{16}ICl_{0.8}$ at $T=4.2$ K.

IV. ANALYSIS

A. First-stage compounds

The increase of the spacing between the graphite layers by the intercalant leads to the formation of a strongly modulated electronic structure along the c axis. In the most simple approximation the first-stage compounds can be considered to consist of a set of equivalent graphite layers (or layered graphite subsystems) without interaction.[1] In this case the dispersion law (in the vicinity of the K point), neglecting spin-orbit interaction, can be written in the form[9]

$$E=\pm\tfrac{3}{2}\gamma_0 b_0 k\ , \tag{1}$$

where γ_0 is a parameter which describes the carbon nearest-neighbor interaction energy, as defined by the resonance integral for the overlap of wave functions at neighboring carbon atoms, $b_0(=1.42$ Å) is the carbon

nearest-neighbor distance, and k is the wave vector. The observation of one single frequency in the SdH signals of the investigated stage-1 compounds is consistent with Eq. (1). The experimental values for the extremal cross section $S_F=\pi k_F^2$ and the effective mass, $m^*=4\hbar^2 E_F/(9\gamma_0^2 b_0^2)$ as determined from the temperature dependence of the SdH oscillations, are listed in Table II. With the value for γ_0 of 3.2 eV, as reported for pure graphite,[10] we have evaluated E_F using Eq. (1) (see Table II). On the other hand, one may also evaluate γ_0 directly from the experimental values of S_F and m^*. However, this results in a value $\gamma_0 \approx 1$ eV, which is much too low and therefore not realistic. This implies that the experimental data of the SdH effect of the first-stage compounds $C_{9.3}AlCl_{3.4}$ and $C_8H_2SO_4$ cannot be described satisfactorily within the simple model proposed by Blinowski *et al.*

B. Second-stage compounds

The second-stage GIC's can, in the most simple approximation, be considered as independent sets of double graphite layers (or graphite subsystems) separated by the intercalant. The band structure consists of two valence and two conduction bands. Blinowski *et al.*[9] derived the following dispersion law (in the vicinity of the K point):

$$E_v^{1,2}=\tfrac{1}{2}\{\pm\gamma_1-\sqrt{\gamma_1^2+3a^2\gamma_0^2k^2}\}\ , \tag{2}$$

where the subscript v refers to the valence bands. Here $a=b_0\sqrt{3}=2.46$ Å is the magnitude of the in-plane translation vector, and γ_1 is a parameter which describes the interaction energy of nearest-neighbor carbon atoms belonging to adjacent graphite layers. This band structure is schematically shown in Fig. 8. The extremal cross sections of the Fermi surface of the two valence bands are given by

$$S^{1,2}=\frac{4\pi}{3a^2\gamma_0^2}|E_F|(|E_F|\pm\gamma_1)\ , \tag{3}$$

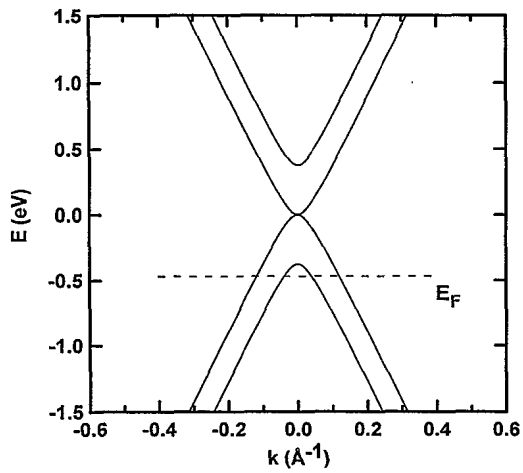

FIG. 8. The band structure of the second-stage $C_{16}ICl_{0.8}$ according to the model by Blinowski *et al.* (Ref. 9). The band-structure parameters derived from the experiments equal $\gamma_0=2.5$ eV and $E_F=-0.47$ eV.

and the effective masses (hole conduction) are given by

$$m^*=\frac{\hbar^2}{2\pi}\frac{\partial S}{\partial E}=\frac{2\hbar^2}{3a^2\gamma_0^2}\left[\gamma_1^2\pm\frac{3a^2\gamma_0^2 S}{\pi}\right]^{1/2}\ . \tag{4}$$

For most of the second-stage compounds we observed only one fundamental frequency in the SdH signals, except in the case of $C_{16}ICl_{0.8}$ (the frequency beats observed in $C_{18.6}AlCl_{3.4}$ will be discussed in Sec. IV C). This implies that for these compounds the Fermi surface consists of one single cylinder. The carriers (holes) occupy the upper valence band only. Using the experimental values for the extremal cross sections and the effective masses (see Table II) we have evaluated γ_0 and E_F with help of Eqs. (2) and (3). For the interaction parameter γ_1, which also defines the energy difference between the two valence bands, we used the value of 0.377 eV reported in Ref. 9. The results are collected in Table II.

The Fourier transform of $C_{16}ICl_{0.8}$ clearly reveals the presence of two frequencies, a low frequency and a high frequency. This shows that the Fermi surface consists of two cylinders. Using the experimental data we calculated the band parameters for the upper and lower bands, while the Fermi energy was adjusted to fit the experimental cross-section areas. The resulting band structure is shown in Fig. 8. The band parameters $\gamma_0=2.5$ eV and $\gamma_1=0.377$ eV give a satisfactory agreement with a value for the Fermi energy of -0.47 eV. The increase in the number of holes in acceptor-type GIC's when compared with graphite results in a stronger screening of the atomic potentials, and reduces the parameter γ_0 with respect to the value for pure graphite (3.2 eV).

C. Undulated cylindrical Fermi surface in $C_{18.6}AlCl_{3.4}$

In the SdH oscillations of the second-stage GIC $C_{18.6}AlCl_{3.4}$ frequency beats are observed in high magnetic fields, yielding two close frequencies. Within the band structure model proposed by Blinowski *et al.*, the Fermi surface consists of either one straight cylinder ($|E_F|<\gamma_1$) or two straight cylinders with distinctly different cross sections ($|E_F|>\gamma_1$). Therefore, the detection of two close frequencies cannot be described with this simple band-structure model. The observed SdH signal can, however, be explained by assuming interlayer interactions resulting in a Fermi surface consisting of an undulating cylinder with two extremal cross sections for a magnetic field applied along the c axis, at $k_z=0$ (the K point of the Brillouin zone) and at $k_z=\pi/I_c$ (the H point). Such an undulating cylindrical Fermi surface was previously detected for the binary intercalated first-stage GIC's $C_{10}CuCl_2ICl_{0.6}$ (Refs. 11 and 12), $C_{15}CuCl_2ICl_{1.2}$ (Refs. 13–15), and $C_{12}FeCl_3ICl_{0.75}$ (Ref. 16), with the help of the SdH effect[11–16] and transport measurements.[11] More recently, an undulated cylindrical Fermi surface was reported[17] for the first-stage GIC $C_{5.5}CdCl_2$.

In considering interlayer interactions, one may assume, in a first approximation, that the energy spectrum of GIC's originates from the graphite energy spectrum.

Within the McClure-Slonczewski-Weiss model for graphite,[18,19] and taking into account only the band parameters γ_0 (nearest-neighbor intralayer interaction) and γ_1 (nearest-neighbor interlayer interaction), the dispersion law for the two valence bands can be written in the form

$$E_{1,2}=\pm\gamma_1^*\cos\phi^*-\sqrt{\gamma_1^{*2}\cos^2\phi^*+\eta^{*2}k^2}\ , \tag{5}$$

where

$$\phi^*=\frac{k_z I_c}{2},\quad \eta^*=\sqrt{3}\frac{a\gamma_0^*}{2}\ . \tag{6}$$

The relevant parameters are now marked by a star in order to distinguish them from the parameters of Eqs. (1)–(3). The main difference between Eqs. (5) and (2) is that in Eq. (5) a k_z dependence is included which results in an undulation of the Fermi surface. The extremal cross sections for the two valence bands at $k_z=0$ are given by

$$S_{1,2}^K=\frac{\pi|E_F|(|E_F|\pm 2\gamma_1^*)}{\eta^{*2}}\ . \tag{7}$$

The effective masses for the two cross sections are

$$m_{1,2}^*=\frac{4\hbar^2}{3a^2\gamma_0^{*2}}(|E_F|\pm\gamma_1^*)\ . \tag{8}$$

Using the experimental value for the extremal cross section of the Fermi surface of the upper valence band at $k_z=0$, $S_F=0.0389$ Å^{-2}, and the experimental value for the effective mass, $m^*/m_0=0.15$, we have evaluated, with the help of Eqs. (7) and (8), values for E_F and γ_0^* where we used a value $\gamma_1^*=\gamma_1=0.377$ eV (see Table II). As $|E_F|(=0.43$ eV) $<2\gamma_1^*$, we did not observe the lower valence band in the SdH signal ($2\gamma_1^*$ is the energy separation between the upper and lower valence band in this model). The experimental Fermi-surface cross section at $k_z=\pi/I_c$ amounts to $S_F=0.0323$ Å^{-2}, which yields an undulation of 17%.

V. DISCUSSION

One of the reasons for the complicated energy spectrum of the GIC's is the possible interaction between carbon atoms in neighboring layers separated by the intercalant layer. Such interactions were conclusively reported[1] to exist in donor-type GIC's. Also, for several acceptor-type GIC's the importance of the interlayer interaction between the carbon atoms was stressed.[20–22] One of the key parameters is the conductivity along the c axis. It is obvious that a cylindrical Fermi surface results in zero electrical conductivity along the c axis, because the hole velocity is perpendicular to the Fermi surface.

The direct interaction between carbon atoms in neighboring layers, described in graphite by the parameter γ_1, is very sensitive to the interlayer distance, and decreases exponentially as this distance increases. The presence of intercalant molecules creates the possibility for some kind of indirect interaction between the carbon atoms separated by the intercalant molecules, by means of overlap between the acceptor and carbon $2p_z$ orbitals. Therefore, it is, strictly speaking, not possible to neglect interlayer interactions for some of the GIC's. Consequently, monointercalated low-stage GIC's also cannot be considered as purely two-dimensional (2D) systems. This phenomenon was previously studied[11–16] in binary intercalated GIC's. The 2D versus 3D character of the system depends on the interlayer spacing and the strength of the interactions between layers. This point was further elucidated by Markiewicz.[20] The crossover from 2D to 3D behavior may explain the existence and peculiarities of the c-axis conductivity in low-stage GIC's.[21,22] Of course, we cannot completely exclude the possibility that the beating in the SdH oscillations for $C_{18.6}AlCl_{3.4}$ arises from sample regions with slightly different concentrations of intercalated molecules and, hence, different concentrations of holes. However, we stress that according to the x-ray data all samples were monophase.

The experimental results indicated that the ratio of the spin to orbital splitting amounts to 0.37 and 0.45 for $C_{9.8}CuCl_2$ and $C_{18.6}AlCl_{3.4}$, respectively. Since $\gamma=gm^*/2m_0$, we conclude that the value of the g factor for holes in GIC's is almost the same as for 2D electrons in GaAs-$Ga_{1-x}Al_xAs$ heterostructures.[23] The enhancement of the g factor in heterostructures was attributed to the exchange interaction of carriers. The same mechanism might be evoked for the quasi-two-dimensional GIC's investigated.

In summary, we have investigated the energy spectrum of various first- and second-stage graphite intercalation compounds by the Shubnikov–de Haas effect, and compared the results with the band-structure model proposed by Blinowski *et al.* A satisfactory agreement is found for the stage-2 compounds only, except in the case of $C_{18.6}AlCl_{3.4}$, where the Fermi surface consists of an undulating cylinder. The undulating Fermi surface can be explained satisfactorily with a band structure adapted from the McClure-Slonczewski-Weiss model, taking into account the energy parameter γ_1^* which describes the interaction between the layers.

ACKNOWLEDGMENTS

Financial support from the International Science Foundation (U.S.A.) and the Russian Foundation for Fundamental Research is gratefully acknowledged. One of us (V.A.K.) is grateful to the University of Amsterdam (UvA) for financial support and hospitality at the Van der Waals–Zeeman Laboratory, offered within the scientific exchange programme UvA-MSU.

*Author to whom correspondence should be addressed. FAX: +31-20-5255788; electronic address: devisser@phys.uva.nl

[1] M. Dresselhaus and G. Dresselhaus, Adv. Phys. **30**, 139 (1981).

[2] See, e.g., *Graphite Intercalation Compounds II: Transport and Electronic Properties,* edited by H. Zabel and S. A. Solin (Springer-Verlag, Berlin, 1992).

[3] See, e.g., D. Shoenberg, *Magnetic Oscillations in Metals* (Cambridge University Press, Cambridge, 1984).

[4]Y. Yosida and S. Tanuma, J. Phys. Soc. Jpn. **54**, 701 (1985).
[5]H. Zalesski, P. K. Ummat, and W. R. Datars, J. Phys. C **17**, 3167 (1984).
[6]H. Zalesski, P. K. Ummat, and W. R. Datars, Phys. Rev. B **35**, 2958 (1987).
[7]G. Wang, P. K. Ummat, and W. R. Datars, Phys. Rev. B **47**, 3864 (1993).
[8]M. Barati, W. R. Datars, P. K. Ummat, and J. Palidwar, Phys. Rev. B **49**, 11 475 (1994).
[9]J. Blinowski, N. H. Hau, C. Rigaux, J. P. Vieren, R. Le Toullec, G. Furdin, A. Hérold, and J. Melin, J. Phys. (Paris) **41**, 47 (1980).
[10]E. Mendez, A. Misu, and M. S. Dresselhaus, Phys. Rev. B **21**, 827 (1980).
[11]V. N. Davydov, V. A. Kulbachinskii, O. M. Nikitina, and V. Ya. Akim, Pis'ma Zh. Eksp. Teor. Fiz. **45**, 567 (1987) [JETP Lett. **45**, 724 (1987)].
[12]V. N. Davydov and V. A. Kulbachinskii, Solid State Commun. **66**, 695 (1988).
[13]V. V. Avdeev, V. Ya. Akim, N. B. Brandt, V. N. Davydov, V. A. Kulbachinskii, and S. G. Ionov, Zh. Eksp. Teor. Fiz. **94**, 188 (1988) [Sov. Phys. JETP **67**, 2496 (1988)].
[14]V. A. Kulbachinskii, Synth. Met. **42**, 2693 (1991).
[15]V. A. Kulbachinskii, N. B. Brandt, N. A. Fadeeva, I. V. Nikolskaya, S. G. Ionov, and V. V. Avdeev, Mater. Sci. Forum **91-93**, 739 (1992).
[16]V. A. Kulbachinskii, S. G. Ionov, S. A. Lapin, and V. V. Avdeev, J. Phys. (France) I **2**, 1941 (1992).
[17]M. Barati, P. K. Ummat, and W. R. Datars, Phys. Rev. B **48**, 15 316 (1993).
[18]J. W. McClure, Phys. Rev. **108**, 612 (1957).
[19]J. W. Slonczewski and P. R. Weiss, Phys. Rev. **109**, 272 (1958).
[20]R. S. Markiewicz, Solid State Commun. **57**, 237 (1986).
[21]E. McRae and J. F. Mareche, J. Mater. Res. **3**, 75 (1988).
[22]O. E. Anderson, B. Sundqvist, E. McRae, J. E. Mareche, and M. Lelaurain, J. Mater. Res. **7**, 2989 (1992).
[23]R. J. Nicholas, M. A. Brummel, J. C. Portal, K. Y. Cheng, A. Y. Cho, and T. P. Pearsell, Solid State Commun. **45**, 911 (1983).